Charge-math xmlns="http://www.w3.org/1998/Math/MathML" display="inline">mn>4/mn>mi>e/mi>/math> Superconductivity from Multicomponent Nematic Pairing: Application to Twisted Bilayer Graphene

Rafael M. Fernandes and Liang Fu

Phys. Rev. Lett. **127**, 047001 — Published 23 July 2021

DOI: 10.1103/PhysRevLett.127.047001

Charge-$4e$ superconductivity from multi-component nematic pairing: Application to twisted bilayer graphene

Rafael M. Fernandes[1] and Liang Fu[2]

[1]School of Physics and Astronomy, University of Minnesota, Minneapolis, Minnesota 55455, USA
[2]Department of Physics, Massachusetts Institute of Technology, Cambridge, MA 02139 USA

(Dated: June 15, 2021)

We show that unconventional nematic superconductors with multi-component order parameter in lattices with three-fold and six-fold rotational symmetries support a charge-$4e$ vestigial superconducting phase above T_c. The charge-$4e$ state, which is a condensate of four-electron bound states that preserve the rotational symmetry of the lattice, is nearly degenerate with a competing vestigial nematic state, which is non-superconducting and breaks the rotational symmetry. This robust result is the consequence of a hidden *discrete* symmetry in the Ginzburg-Landau theory, which permutes quantities in the gauge sector and in the crystalline sector of the symmetry group. We argue that random strain generally favors the charge-$4e$ state over the nematic phase, as it acts as a random-mass to the former but as a random-field to the latter. Thus, we propose that two-dimensional inhomogeneous systems displaying nematic superconductivity, such as twisted bilayer graphene, provide a promising platform to realize the elusive charge-$4e$ superconducting phase.

Introduction. The collective behavior of interacting electrons in quantum materials can give rise to a plethora of exotic phenomena. An interesting example is charge-$4e$ superconductivity [1–13], an intriguing macroscopic quantum phenomena which was theoretically proposed but is yet to be observed. In contrast to standard charge-$2e$ superconductors characterized by Cooper pairing, a charge-$4e$ superconductor is formed by the condensation of four-electron bound states. Many basic properties of this exotic state, such as whether its quasi-particle excitation spectrum is gapless or gapped, remain under debate [12].

One strategy to search for charge-$4e$ superconductivity is to look for systems that display two condensates, and search for a stable state where pairs of Cooper pairs are formed even in the absence of phase coherence among the Cooper pairs. One widely explored option is the so-called pair-density wave (PDW) state, in which the Cooper pairs have a finite center-of-mass momentum [13]. An unidirectional PDW is described by two complex gap functions $\Delta_{\pm\mathbf{Q}}$ that have incommensurate ordering vectors $\pm\mathbf{Q}$. Charge-$4e$ superconductivity, described by the composite order parameter $\Delta_{\mathbf{Q}}\Delta_{-\mathbf{Q}}$, is a secondary order that exists inside the PDW state. It has been proposed that the PDW state can melt in two stages before reaching the normal state [6], giving rise to an intermediate state in which there is no PDW order, $\langle\Delta_{\pm\mathbf{Q}}\rangle = 0$, but there is charge-$4e$ superconducting order, $\langle\Delta_{\mathbf{Q}}\Delta_{-\mathbf{Q}}\rangle \neq 0$. Such an intermediate phase is called a vestigial phase [14–16], as it breaks a subset of the symmetries broken in the primary PDW state. The main drawback of this interesting idea is the fact that the occurrence of PDW states in actual materials and in microscopic models seems to be rather rare [13]. Thus, it is desirable to search for other systems that may host vestigial charge-$4e$ superconductivity.

In this paper, we show that nematic superconductors in hexagonal and trigonal lattices offer a promising alternative. A nematic superconductor breaks both the gauge symmetry associated with the phase of the gap function and the three-fold/six-fold rotational symmetry of the lattice. Importantly, nematic superconductivity has been experimentally observed in doped Bi_2Se_3 [17, 18] and in twisted bilayer graphene [19], two systems whose lattices have three-fold rotational symmetry. Superconducting properties that do not respect the three-fold lattice symmetry were also observed in few-layer $NbSe_2$, although it is unclear whether this is a consequence of a nematic pair-

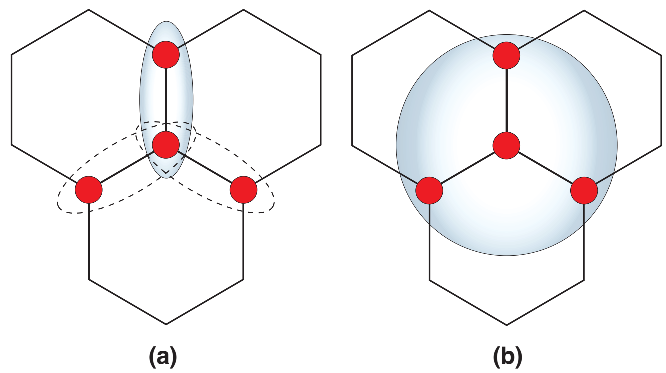

FIG. 1. A nematic superconducting state in a lattice with three-fold or six-fold rotational symmetry (here, a honeycomb lattice is shown) is described by a two-component order parameter $(\Delta_1, \Delta_2) = \Delta_0(\cos\theta, \sin\theta)$, represented here by bound states of electron pairs (red dots). The ellipses represent, schematically, different orientations θ. Two competing vestigial phases are supported: (a) a Potts-nematic phase and (b) a charge-$4e$ phase. In (a), the angle θ associated with the nematic director is fixed, breaking the three-fold rotational symmetry. In (b), the three-fold rotational symmetry is preserved and a coherent state of bound states of four electrons emerge. In both (a) and (b), $\langle\Delta_i\rangle = 0$, i.e. charge-$2e$ superconducting order is absent.

ing state [20, 21]. Unless finite tuning is invoked [22, 23], nematic superconductivity is realized in systems where the order parameter transforms as a multi-dimensional irreducible representation of the relevant point group G [19, 24–28]. Typical examples are two-dimensional representations $(\Delta_1,\,\Delta_2)$ where Δ_1 and Δ_2 correspond to p_x-wave/p_y-wave gaps or $d_{x^2-y^2}$-wave/d_{xy}-wave gaps. Interestingly, it has been shown that a secondary composite order parameter $\mathbf{\Phi}=\left(\left|\Delta_1\right|^2-\left|\Delta_2\right|^2,-\Delta_1\Delta_2^*-\Delta_1^*\Delta_2\right)$, corresponding to Potts-nematic order, can onset even above the superconducting transition temperature T_c [26, 29].

Here, we show that the very same mechanism that favors a vestigial nematic phase also promotes a vestigial charge-4e phase characterized by a non-zero composite order parameter $\psi=\Delta_1^2+\Delta_2^2$, but $\langle\Delta_i\rangle=0$ (see Fig. 1). In particular, we find that the effective Ginzburg-Landau theory obtained after integrating out the normal-state superconducting fluctuations has the same form for both the nematic order parameter $\mathbf{\Phi}$ and the charge-4e order parameter ψ. We show that this is a robust result stemming from the existence of a linear transformation, called a *perfect shuffle permutation*, that relates $\mathbf{\Phi}$ and ψ in the four-dimensional space spanned by Δ_1 and Δ_2. Such a transformation effectively permutes quantities in the "gauge sector" and in the "crystalline sector" of the group $\mathrm{U}(1)\otimes G$ that defines the symmetry properties of the system.

This result implies that there are actually two competing vestigial phases that can onset before long-range superconductivity sets in: nematic order, as studied previously [26, 29], and charge-4e superconductivity. While additional terms in the superconducting free-energy can favor either state, the coupling to random strain fundamentally alters the balance between them. This is because random strain acts as a random-field to $\mathbf{\Phi}$, but as a random-mass to ψ. Consequently, random strain, intrinsically present in actual materials, is expected to suppress Potts-nematic order much more strongly than charge-4e order. We thus conclude that the most promising candidates to realize vestigial charge-4e superconductivity are relatively inhomogeneous nematic superconductors with strong superconducting fluctuations, as in quasi-2D systems. This analysis thus suggests that twisted bilayer graphene [30–38] offers a potentially viable platform to realize this elusive state of matter.

Vestigial nematicity: the standard scenario. We consider a nematic superconductor in a lattice with three-fold or six-fold rotational symmetry, described by a two-component order parameter $(\Delta_1,\,\Delta_2)$. For concreteness, hereafter we will focus on the case where the point group of the lattice is D_6, and $\mathbf{\Delta}\equiv(\Delta_1,\,\Delta_2)^\dagger$ transforms as the E_2 irreducible representation (irrep), corresponding to $\left(d_{x^2-y^2},\,d_{xy}\right)$-wave gaps. Note, our results also apply to $\mathbf{\Delta}$ transforming as two-dimensional E-like irreps of D_6, D_3, C_{3v}, etc. The Ginzburg-Landau superconducting action expanded to fourth order in $\mathbf{\Delta}$ is given by [22, 26, 29, 39]:

$$S\left[\mathbf{\Delta}\right]=\int_q\Delta_{i,q}^*\chi_{ij}^{-1}\left(q\right)\Delta_{j,q}+\frac{u_0}{2}\int_r\left(\left|\Delta_1\right|^2+\left|\Delta_2\right|^2\right)^2+\frac{\gamma}{2}\int_r\left|\Delta_1\Delta_2^*-\Delta_1^*\Delta_2\right|^2 \qquad (1)$$

Here, $\chi_{ij}^{-1}\left(q\right)$ is the inverse superconducting susceptibility in Fourier space, whereas $u_0>0$ and γ are Ginzburg-Landau parameters. Furthermore, $q=(\mathbf{q},\omega_n)$ and $r=(\mathbf{r},\tau)$, where $\mathbf{q}$ is the momentum, ω_n is the bosonic Matsubara frequency, $\mathbf{r}$ is the position, and τ is the imaginary time. Note that S has an enlarged continuous rotational symmetry $\Delta_1\pm i\Delta_2\to e^{\pm i\theta}(\Delta_1\pm i\Delta_2)$, which is reduced to a discrete one when higher-order terms are included, as we discuss later.

The superconducting ground state depends on γ: if $\gamma<0$, the action is minimized by $\mathbf{\Delta}=\Delta_0\left(1,\,\pm i\right)^\dagger$, corresponding to a time-reversal symmetry-breaking (TRSB) superconductor that preserves the six-fold rotational symmetry of the lattice. If $\gamma>0$, we obtain $\mathbf{\Delta}=\Delta_0\left(\cos\theta,\,\sin\theta\right)^\dagger$, with arbitrary θ, corresponding to a nematic pairing state, as it preserves time-reversal symmetry but lowers the six-fold rotational symmetry to two-fold. It is convenient to construct the real-valued composite order parameters $\zeta\equiv\mathbf{\Delta}^\dagger\sigma^y\mathbf{\Delta}$ and $\mathbf{\Phi}\equiv\left(\mathbf{\Delta}^\dagger\sigma^z\mathbf{\Delta},\,-\mathbf{\Delta}^\dagger\sigma^x\mathbf{\Delta}\right)$, where σ^μ is a Pauli matrix that acts on the two-dimensional subspace spanned by $\mathbf{\Delta}$ [16, 26, 29]. While ζ transforms as the A_2 irrep of D_6, and is thus related to TRSB, $\mathbf{\Phi}$ transforms as the E_2 irrep, being related to six-fold rotational symmetry breaking. Clearly, if the ground state is $\mathbf{\Delta}=\Delta_0\left(1,\,\pm i\right)^\dagger$, $\zeta\neq0$ and $\mathbf{\Phi}=0$, but if $\mathbf{\Delta}=\Delta_0\left(\cos\theta,\,\sin\theta\right)^\dagger$, $\zeta=0$ and $\mathbf{\Phi}\neq0$. The sign of γ is ultimately determined by microscopic considerations. While weak-coupling calculations favor $\gamma<0$ [22, 28, 40], spin-orbit coupling or density-wave/nematic fluctuations favor the nematic superconducting state [24, 25, 28, 41]. Hereafter, we will assume one of these microscopic mechanisms as the source of $\gamma>0$.

The nematic superconducting state supports a vestigial nematic phase, i.e. a phase in which the composite nematic order parameter is non-zero, $\langle\mathbf{\Phi}\rangle\neq0$, but superconducting order is absent, $\langle\mathbf{\Delta}\rangle=0$ (see Fig. 1(a)). To see this, we follow Ref. [16] and rewrite the quartic terms in Eq. (1) in terms of the TRSB bilinear $\zeta=\mathbf{\Delta}^\dagger\sigma^y\mathbf{\Delta}$ and the trivial bilinear $\lambda\equiv\mathbf{\Delta}^\dagger\sigma^0\mathbf{\Delta}$ as $S^{(4)}=\frac{u_0}{2}\int_r\lambda^2+\frac{\gamma}{2}\int_r\zeta^2$. Here, σ^0 is the identity matrix. Now, the Fierz identity $\sum_\mu\sigma_{ij}^\mu\sigma_{kl}^\mu=2\delta_{il}\delta_{jk}-\sigma_{ij}^0\sigma_{kl}^0$ implies a relationship between the bilinears, $\zeta^2=\lambda^2-\Phi^2$. As a result, the quartic term can be rewritten as $S^{(4)}=\frac{u}{2}\int_r\lambda^2-\frac{\gamma}{2}\int_r\Phi^2$, where $u\equiv u_0+\gamma$ and, as defined above, $\mathbf{\Phi}=(\Phi_1,\Phi_2)=\left(\mathbf{\Delta}^\dagger\sigma^z\mathbf{\Delta},\,-\mathbf{\Delta}^\dagger\sigma^x\mathbf{\Delta}\right)$ is the nematic bilinear. Since $\gamma > 0$ by assumption, we can perform Hubbard-Stratonovich transformations to decouple the quartic terms and obtain:

$$S[\mathbf{\Delta},\lambda,\mathbf{\Phi}] = \int_r \frac{\Phi^2}{2\gamma} - \int_r \frac{\lambda^2}{2u} + \int_q \Delta^*_{i,q}\left[\chi^{-1}_{ij}(q) + \lambda\sigma^0_{ij} - \Phi_1\sigma^z_{ij} + \Phi_2\sigma^x_{ij}\right]\Delta_{j,q} \quad (2)$$

Because the action is quadratic in Δ_i, superconducting fluctuations can be exactly integrated out in the normal state, yielding an effective action for $\mathbf{\Phi}$ and λ . Since λ does not break any symmetries, it is always non-zero and simply renormalizes the static superconducting susceptibility. On the other hand, $\mathbf{\Phi}$ is only non-zero below an onset temperature. A large-N calculation [42], as performed in Ref. [29], indicates that $\langle\mathbf{\Phi}\rangle \neq 0$ already above T_c, implying that vestigial nematic order precedes the onset of superconductivity (see also the Supplementary Material, SM [43]). Interestingly, a vestigial nematic phase has been recently observed in doped Bi_2Se_3 [44, 45].

Competition between nematicity and charge-4e superconductivity. We now show that there is a hidden symmetry between the two-component real-valued nematic order parameter $\mathbf{\Phi}$ and the complex bilinear $\psi \equiv \Delta_1^2 + \Delta_2^2$. The latter, which is non-zero (zero) inside the nematic (TRSB) superconducting state, breaks the U(1) gauge symmetry and is precisely the charge-$4e$ order parameter (see Fig. 1(b)). To reveal this unexpected symmetry, we construct complex bilinears out of the primary order parameter $\mathbf{\Delta}$. Since the latter transforms as the irrep $\Gamma = \mathrm{e}^{im\theta} \otimes E_2$ of the group $\mathrm{U}(1) \otimes D_6$, we can write it as a four-dimensional vector $\boldsymbol{\eta} \equiv (\Delta_1', \Delta_1'', \Delta_2', \Delta_2'')^T$, where the prime (double prime) denotes the real (imaginary) part. Then, the bilinears are generally given by $\boldsymbol{\eta}^T(\sigma^\mu \otimes \sigma^m)\boldsymbol{\eta}$, where the first Pauli matrix (with Greek superscript) in the Kronecker product $\sigma^\mu \otimes \sigma^m$ refers to the subspace associated with the two-dimensional irrep E_2 (dubbed the crystalline sector), whereas the second Pauli matrix (with Latin superscript) refers to the subspace associated with the U(1) group (dubbed the gauge sector). In this notation, the components of the nematic bilinear become:

$$\Phi_1 = \boldsymbol{\eta}^T\left(\sigma^z \otimes \sigma^0\right)\boldsymbol{\eta}$$
$$\Phi_2 = -\boldsymbol{\eta}^T\left(\sigma^x \otimes \sigma^0\right)\boldsymbol{\eta} \quad (3)$$

The other real bilinears are given by $\zeta = \boldsymbol{\eta}^T(\sigma^y \otimes \sigma^y)\boldsymbol{\eta}$ and $\lambda = \boldsymbol{\eta}^T(\sigma^0 \otimes \sigma^0)\boldsymbol{\eta}$. The charge-$4e$ bilinear $\psi \equiv \psi' + i\psi''$, on the other hand, is:

$$\psi' = \boldsymbol{\eta}^T\left(\sigma^0 \otimes \sigma^z\right)\boldsymbol{\eta}$$
$$\psi'' = \boldsymbol{\eta}^T\left(\sigma^0 \otimes \sigma^x\right)\boldsymbol{\eta} \quad (4)$$

The key point is that, although the Kronecker product $(M \otimes N)$ is non-commutative, in the case where M and N are square matrices it satisfies the property $(M \otimes N) = \tilde{P}^T(N \otimes M)\tilde{P}$, where $\tilde{P}$ is the so-called *perfect shuffle permutation matrix* [46]. Here, due to the minus sign in the second equation of (3), a slightly modified 2×2 matrix P is needed:

$$P = \begin{pmatrix} 1 & 0 & 0 & 0 \\ 0 & 0 & -1 & 0 \\ 0 & -1 & 0 & 0 \\ 0 & 0 & 0 & 1 \end{pmatrix} \quad (5)$$

Physically, P permutes quantities from the crystalline and the gauge sectors of the four-dimensional space spanned by $\boldsymbol{\eta}$. Because P is an orthogonal matrix, $P^{-1} = P^T = P$, upon performing the unitary transformation $\tilde{\boldsymbol{\eta}} = P\boldsymbol{\eta}$, we see that while the bilinears ζ and λ remain invariant, $(\Phi_1, \Phi_2) \to (\psi', \psi'')$, i.e. the nematic bilinear is mapped onto the charge-$4e$ bilinear. Consequently, provided that the susceptibility in the quadratic term of Eq. (1) is invariant under the linear transformation (5), the effective action in the normal state has the same functional form with respect to either Φ^2 or $|\psi|^2$. This is the case if we consider the standard susceptibility expression $\chi^{-1}_{ij}(q) = \left(r_0 + q^2\right)\delta_{ij}$, where $r_0 \propto T - T_{c,0}$ is a tuning parameter and $T_{c,0}$ is the bare superconducting transition temperature (see the SM).

This is the main result of our paper: for the Ginzburg-Landau action in Eq. (1), which describes a nematic superconducting ground state in a lattice with three-fold or six-fold rotational symmetry, an instability towards a vestigial nematic state at T_{nem} implies an instability towards a vestigial charge-$4e$ state at the same temperature $T_{4e} = T_{\mathrm{nem}}$. This degeneracy between nematicity and charge-$4e$ superconductivity is rooted on the invariance of the action upon a perfect shuffle that permutes elements from the crystalline and the gauge sectors. As we show in the SM, an explicit large-N calculation shows that, for anisotropic 2D systems, there is a wide parameter regime for which $T_{4e} = T_{\mathrm{nem}} > T_c$, implying that the vestigial order emerges before the onset of superconductivity.

Selecting nematic or charge-4e order. We proceed to discuss how the degeneracy between charge-$4e$ and nematicity is lifted. Focusing on finite-temperature phase transitions, two additional terms in the superconducting action (1), not considered in the analysis above, break the degeneracy in different ways. The first one is a symmetry-allowed anisotropic term in $\chi^{-1}_{ij}(q)$ of the form $\kappa\left[\left(q_x^2 - q_y^2\right)\left(\sigma^z \otimes \sigma^0\right)_{ij} + 2q_xq_y\left(\sigma^x \otimes \sigma^0\right)_{ij}\right]$, with coefficient κ. Within large-N, this contribution gives $T_{4e} > T_{\mathrm{nem}}$, as we show in the SM. The second one is the sixth-order term [39]:

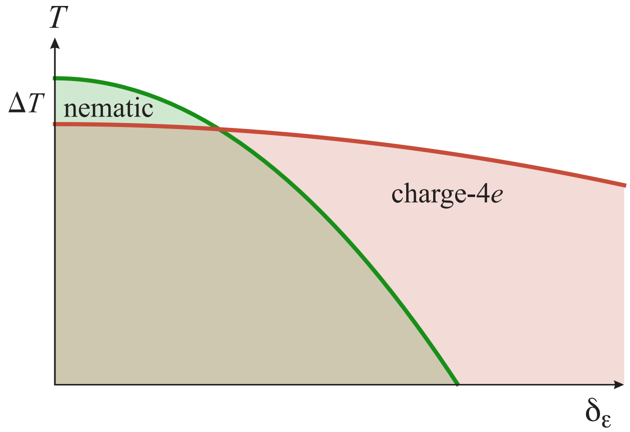

FIG. 2. Schematic phase diagram of the vestigial nematic (transition temperature T_{nem}, green) and vestigial charge-4e (T_{4e}, red) phases. Here, δ_ε represents the strength of strain inhomogeneity. Because random strain couples as a random-field to the nematic order parameter but as a random-mass to the charge-4e order parameter, the former is expected to be suppressed much more strongly than the latter. In the clean system, $\Delta T \equiv T_{\mathrm{nem}} - T_{4e}$ is positive because of the sixth-order term in Eq. (6) that restricts the nematic director to three directions (3-state Potts nematicity) and lifts the emergent degeneracy between the two vestigial ordered phases. Note that, as temperature is lowered, a superconducting transition is expected (not shown here). Whether charge-4e and nematic orders can coexist in the overlapping region of the phase diagram remains to be studied.

$$S^{(6)}\left[\mathbf{\Delta}\right] = \rho \int_r \left[\left(\Delta_1 + i\Delta_2\right)^3 \left(\Delta_1^* + i\Delta_2^*\right)^3 + \text{h.c.} \right] \quad (6)$$

Here, ρ is a coupling constant. Expressed in terms of the nematic bilinear $\mathbf{\Phi}$, it corresponds to a symmetry-allowed cubic term in the nematic action proportional to $\left(\Phi_+^3 + \Phi_-^3\right)$, where $\Phi_\pm = \Phi_1 \pm i\Phi_2$ [24, 26, 29, 47, 48]. In contrast, because ψ is complex, such a cubic term is not allowed in the charge-4e action. This cubic term lowers the symmetry of the nematic order parameter from continuous U(1) to discrete 3-state Potts, as it fixes the phase of $\Phi_\pm$ to three possible values [26, 29, 47, 49]. Moreover, it gives $T_{\mathrm{nem}} > T_{4e}$, as shown by a mean-field calculation (see SM). Thus, depending on which of the effects associated with the coupling constants κ and ρ is stronger, either a vestigial nematic or a vestigial charge-4e order can be favored.

There is, however, an important ingredient missing in our analysis that generally favors the charge-4e instability, thus opening a route to realize this exotic state in realistic settings: the coupling to lattice degrees of freedom. The latter are described by the strain tensor $\varepsilon_{ij} = \frac{1}{2}\left(\partial_i u_j + \partial_j u_i\right)$, with $\mathbf{u}$ denoting the lattice displacement vector. Decomposing it in the irreps of the D_6 group, there are two relevant modes: the longitudinal mode, which transforms as A_1, $\varepsilon_A \equiv \varepsilon_{xx} + \varepsilon_{yy} + \varepsilon_{zz}$, and the shear mode, which transforms as E_2, $\boldsymbol{\varepsilon}_E \equiv \left(\varepsilon_{xx} - \varepsilon_{yy},\, -2\varepsilon_{xy}\right)$. As a result, the leading-order couplings to the nematic and charge-4e orders are given, respectively, by the linear coupling $\boldsymbol{\varepsilon}_E \cdot \mathbf{\Phi}$ and by the quadratic coupling $\varepsilon_A \left|\psi\right|^2$. Thus, uniaxial strain acts as a conjugate field to the nematic order parameter – a well-known result [48] – whereas for the charge-4e order parameter, it can only change the transition temperature, similarly to hydrostatic pressure.

While strain can be externally applied, it is intrinsically present in materials as random strain caused by defects arising in the crystal growth or device fabrication. From the analysis above, it is clear that such random strain acts as a random-field to the Potts-nematic order parameter, but as a random-mass (also called random-T_c) to the charge-4e order parameter. This distinction is very important, as random-field disorder is known to be much more detrimental to long-order range order than random-mass disorder. For the 3-state Potts model, random-field is believed to completely kill the Potts transition in two dimensions, and to suppress it in three dimensions [50–52]. In the 2D case, the situation is similar to the random-field Ising model (see e.g. [53]): random-strain breaks up the Potts-nematic ordered state into multiple domains, destroying long-range order. The so-called breakup length L_b characterizing these domains depends on the width $\delta\varepsilon$ of the distribution of random strains according to $L_b \sim \exp\left(B/\delta\varepsilon^2\right)$ (see SM for details). Consequently, in 2D, even an infinitesimal strain inhomogeneity $\delta\varepsilon$ kills nematic order in the thermodynamic limit. Thus, one generally expects random strain to tilt the balance between the competing vestigial charge-4e and nematic orders in favor of the former. The resulting schematic phase diagram is shown in Fig. 2.

Experimental consequences. Nematic superconductivity has been now established in doped Bi_2Se_3 and in twisted bilayer graphene (TBG) [17–19]. The latter seems to be the most promising candidate to realize our results. First, TBG displays 2D superconductivity, and fluctuations are stronger in low-dimensional superconductors. Second, its superconducting state breaks three-fold rotational symmetry in different directions over a range of carrier concentrations [19], indicative of $\gamma > 0$ in (1). Third, strain inhomogeneities in TBG appear to be strong enough to suppress nematic order. A good proxy for strain inhomogeneity is the width $\delta\varepsilon$ of the distribution of local strains. Because the moiré lattice parameter a_M of TBG is very large, a typical device has a linear size $L \sim 100 a_M$. This defines a critical inhomogeneity strength $\delta\varepsilon_c$ beyond which the breakup length L_b discussed above is smaller than L, and nematic order is destroyed. We estimate $\delta\varepsilon_c \approx 0.2\, T_c/\zeta_{\mathrm{nem-el}}$, where $T_c \sim 3$ K is the typical TBG superconducting transition temperature and $\zeta_{\mathrm{nem-el}}$ is the nemato-elastic coupling (see SM). Experimental measurements of heterostrain in

TBG find local strain values as big as 0.4%, and a distribution of strains with large standard deviations, of about 50% of the average value [54, 55]. This strain inhomogeneity is also reflected in a twist angle inhomogeneity, which has been widely studied in TBG [56–59].

Therefore, as long as the nemato-elastic coupling is not too small, inhomogeneous TBG devices in the doping range where nematic superconductivity is found are promising candidates to realize charge-$4e$ order. Note that the mechanism proposed here is different from a recent proposal for charge-$4e$ superconductivity based on an approximate SU(4) symmetry of twisted bilayer graphene [60]. To experimentally detect charge-$4e$ order, one would search for signatures of vortices with half quantum flux ($hc/4e$), for instance in phase-sensitive experiments involving Josephson junctions, such as the SQUID loop proposed in Ref. [6]. Alternatively, atomically-resolved shot noise measurements using Josephson scanning tunneling microscopy, such as those performed in Ref. [61], could also be used to directly detect the charge-$4e$ bound state.

Conclusions. In this paper, we showed that a nematic superconductor in lattices with three-fold or six-fold rotational symmetry supports competing nematic and charge-$4e$ vestigial orders. Such a competition is rooted on a perfect shuffle permutation that transforms one order parameter onto the other in the four-dimensional space spanned by the multi-component superconducting order parameter. We showed that random strain provides the most promising tuning knob to favor charge-$4e$ superconductivity over nematic order, due to the fact that it acts as a random-field disorder to the latter, but as a random-mass disorder to the latter. These results establish a new class of systems – nematic superconductors – in which charge-$4e$ order may be realized.

We thank A. Chubukov, P. Orth, J. Schmalian, and J. Venderbos for fruitful discussions. This work was supported by the U. S. Department of Energy, Office of Science, Basic Energy Sciences, Materials Sciences and Engineering Division, under Award No. DE-SC0020045 (R.M.F.) and DE-SC0018945 (L.F.).

[1] S. Korshunov, Zh. Eksp. Teor. Fiz **89**, 539 (1985).
[2] G. E. Volovik, *Exotic properties of superfluid 3He*, vol. 1 (World Scientific, 1992).
[3] G. Röpke, A. Schnell, P. Schuck, and P. Nozières, Phys. Rev. Lett. **80**, 3177 (1998).
[4] C. Wu, Phys. Rev. Lett. **95**, 266404 (2005).
[5] A. A. Aligia, A. P. Kampf, and J. Mannhart, Phys. Rev. Lett. **94**, 247004 (2005).
[6] E. Berg, E. Fradkin, and S. A. Kivelson, Nature Phys. **5**, 830 (2009).
[7] L. Radzihovsky and A. Vishwanath, Phys. Rev. Lett. **103**, 010404 (2009).
[8] E. V. Herland, E. Babaev, and A. Sudbø, Phys. Rev. B **82**, 134511 (2010).
[9] D. F. Agterberg, M. Geracie, and H. Tsunetsugu, Phys. Rev. B **84**, 014513 (2011).
[10] L. Radzihovsky, Phys. Rev. A **84**, 023611 (2011).
[11] E.-G. Moon, Phys. Rev. B **85**, 245123 (2012).
[12] Y.-F. Jiang, Z.-X. Li, S. A. Kivelson, and H. Yao, Phys. Rev. B **95**, 241103 (2017).
[13] D. F. Agterberg, J. S. Davis, S. D. Edkins, E. Fradkin, D. J. Van Harlingen, S. A. Kivelson, P. A. Lee, L. Radzihovsky, J. M. Tranquada, and Y. Wang, Annual Review of Condensed Matter Physics **11**, 231 (2020).
[14] L. Nie, G. Tarjus, and S. A. Kivelson, Proceedings of the National Academy of Sciences **111**, 7980 (2014).
[15] E. Fradkin, S. A. Kivelson, and J. M. Tranquada, Rev. Mod. Phys. **87**, 457 (2015).
[16] R. M. Fernandes, P. P. Orth, and J. Schmalian, Annual Review of Condensed Matter Physics **10**, 133 (2019).
[17] K. Matano, M. Kriener, K. Segawa, Y. Ando, and G.-q. Zheng, Nature Phys. **12**, 852 (2016).
[18] S. Yonezawa, K. Tajiri, S. Nakata, Y. Nagai, Z. Wang, K. Segawa, Y. Ando, and Y. Maeno, Nature Phys. **13**, 123 (2017).
[19] Y. Cao, D. Rodan-Legrain, J. M. Park, N. F. Q. Yuan, K. Watanabe, T. Taniguchi, R. M. Fernandes, L. Fu, and P. Jarillo-Herrero, Science **372**, 264 (2021).
[20] A. Hamill, B. Heischmidt, E. Sohn, D. Shaffer, K.-T. Tsai, X. Zhang, X. Xi, A. Suslov, H. Berger, L. Forró, et al., arXiv:2004.02999 (2020).
[21] C.-w. Cho, J. Lyu, T. Han, C. Y. Ng, Y. Gao, G. Li, M. Huang, N. Wang, and R. Lortz, arXiv:2003.12467 (2020).
[22] D. V. Chichinadze, L. Classen, and A. V. Chubukov, Phys. Rev. B **101**, 224513 (2020).
[23] Y. Wang, J. Kang, and R. M. Fernandes, arXiv:2009.01237 (2020).
[24] L. Fu, Phys. Rev. B **90**, 100509 (2014).
[25] J. W. F. Venderbos, V. Kozii, and L. Fu, Phys. Rev. B **94**, 180504 (2016).
[26] J. W. F. Venderbos and R. M. Fernandes, Phys. Rev. B **98**, 245103 (2018).
[27] Y. Su and S.-Z. Lin, Phys. Rev. B **98**, 195101 (2018).
[28] V. Kozii, H. Isobe, J. W. F. Venderbos, and L. Fu, Phys. Rev. B **99**, 144507 (2019).
[29] M. Hecker and J. Schmalian, npj Quantum Materials **3**, 26 (2018).
[30] Y. Cao, V. Fatemi, S. Fang, K. Watanabe, T. Taniguchi, E. Kaxiras, and P. Jarillo-Herrero, Nature **556**, 43 (2018).
[31] Y. Cao, V. Fatemi, A. Demir, S. Fang, S. L. Tomarken, J. Y. Luo, J. D. Sanchez-Yamagishi, K. Watanabe, T. Taniguchi, E. Kaxiras, et al., Nature **556**, 80 (2018).
[32] M. Yankowitz, S. Chen, H. Polshyn, Y. Zhang, K. Watanabe, T. Taniguchi, D. Graf, A. F. Young, and C. R. Dean, Science **363**, 1059 (2019).
[33] X. Lu, P. Stepanov, W. Yang, M. Xie, M. A. Aamir, I. Das, C. Urgell, K. Watanabe, T. Taniguchi, G. Zhang, et al., Nature **574**, 653 (2019).
[34] A. L. Sharpe, E. J. Fox, A. W. Barnard, J. Finney, K. Watanabe, T. Taniguchi, M. A. Kastner, and D. Goldhaber-Gordon, Science **365**, 605 (2019).
[35] A. Kerelsky, L. J. McGilly, D. M. Kennes, L. Xian, M. Yankowitz, S. Chen, K. Watanabe, T. Taniguchi, J. Hone, C. Dean, et al., Nature **572**, 95 (2019).
[36] Y. Jiang, X. Lai, K. Watanabe, T. Taniguchi, K. Haule,

J. Mao, and E. Y. Andrei, Nature **573**, 91 (2019).

[37] Y. Choi, J. Kemmer, Y. Peng, A. Thomson, H. Arora, R. Polski, Y. Zhang, H. Ren, J. Alicea, G. Refael, et al., Nature Physics **15**, 1174 (2019).

[38] Y. Xie, B. Lian, B. Jäck, X. Liu, C.-L. Chiu, K. Watanabe, T. Taniguchi, B. A. Bernevig, and A. Yazdani, Nature **572**, 101 (2019).

[39] M. Sigrist and K. Ueda, Rev. Mod. Phys. **63**, 239 (1991).

[40] R. Nandkishore, L. Levitov, and A. Chubukov, Nature Phys. **8**, 158 (2012).

[41] R. M. Fernandes and A. J. Millis, Phys. Rev. Lett. **111**, 127001 (2013).

[42] R. M. Fernandes, A. V. Chubukov, J. Knolle, I. Eremin, and J. Schmalian, Phys. Rev. B **85**, 024534 (2012).

[43] See Supplementary Material, which also includes Refs. [62] and [63], for the detailed derivation of the large-N effective action, comparison between the transition temperatures, and discussion of the effective random-field Potts model.

[44] Y. Sun, S. Kittaka, T. Sakakibara, K. Machida, J. Wang, J. Wen, X. Xing, Z. Shi, and T. Tamegai, Phys. Rev. Lett. **123**, 027002 (2019).

[45] C.-w. Cho, J. Shen, J. Lyu, O. Atanov, Q. Chen, S. H. Lee, Y. San Hor, D. J. Gawryluk, E. Pomjakushina, M. Bartkowiak, et al., Nature communications **11**, 1 (2020).

[46] M. Davio, IEEE Transactions on Computers **100**, 116 (1981).

[47] Y. Xu, X.-C. Wu, C.-M. Jian, and C. Xu, Phys. Rev. B **101**, 205426 (2020).

[48] R. M. Fernandes and J. W. F. Venderbos, Science Advances **6**, eaba8834 (2020).

[49] S. Jin, W. Zhang, X. Guo, X. Chen, X. Zhou, and X. Li, arXiv:1910.11880 (2019).

[50] D. Blankschtein, Y. Shapir, and A. Aharony, Phys. Rev. B **29**, 1263 (1984).

[51] K. Eichhorn and K. Binder, Journal of Physics: Condensed Matter **8**, 5209 (1996).

[52] M. Kumar, R. Kumar, M. Weigel, V. Banerjee, W. Janke, and S. Puri, Phys. Rev. E **97**, 053307 (2018).

[53] E. T. Seppälä, V. Petäjä, and M. J. Alava, Phys. Rev. E **58**, R5217 (1998).

[54] T. Benschop, T. A. de Jong, P. Stepanov, X. Lu, V. Stalman, S. J. van der Molen, D. K. Efetov, and M. P. Allan, Phys. Rev. Research **3**, 013153 (2021).

[55] N. P. Kazmierczak, M. Van Winkle, C. Ophus, K. C. Bustillo, S. Carr, H. G. Brown, J. Ciston, T. Taniguchi, K. Watanabe, and D. K. Bediako, Nature Materials (2021), URL https://doi.org/10.1038/s41563-021-00973-w.

[56] A. Uri, S. Grover, Y. Cao, J. Crosse, K. Bagani, D. Rodan-Legrain, Y. Myasoedov, K. Watanabe, T. Taniguchi, P. Moon, et al., Nature **581**, 47 (2020).

[57] J. H. Wilson, Y. Fu, S. Das Sarma, and J. H. Pixley, Phys. Rev. Research **2**, 023325 (2020).

[58] B. Padhi, A. Tiwari, T. Neupert, and S. Ryu, Phys. Rev. Research **2**, 033458 (2020).

[59] C. Tschirhart, M. Serlin, H. Polshyn, A. Shragai, Z. Xia, J. Zhu, Y. Zhang, K. Watanabe, T. Taniguchi, M. Huber, et al., arXiv:2006.08053 (2020).

[60] E. Khalaf, P. Ledwith, and A. Vishwanath, arXiv:2012.05915 (2020).

[61] K. M. Bastiaans, D. Cho, D. Chatzopoulos, M. Leeuwenhoek, C. Koks, and M. P. Allan, Phys. Rev. B **100**, 104506 (2019).

[62] J. W. F. Venderbos, V. Kozii, and L. Fu, Phys. Rev. B **94**, 094522 (2016).

[63] M. E. Fisher, Reports on Progress in Physics **30**, 615 (1967).